CIDNP and EPR Study of Phototransformation of Lappaconitine Derivatives in Solution

Nikolay E. Polyakov,*,† Olga A. Simaeva,† Marc B. Taraban,† Tatyana V. Leshina,† Tatyana A. Konovalova,‡ Lowell D. Kispert,‡ Irina A. Nikitina,§,# Natalia A. Pankrushina,§,# and Alexey V. Tkachev§

Institute of Chemical Kinetics & Combustion, Institutskaya Str. 3, 630090, Novosibirsk, Russia, Chemistry Department, University of Alabama, Tuscaloosa, Alabama 35487-0336, Novosibirsk Institute of Organic Chemistry, Lavrentiev Ave. 9, 630090, Novosibirsk, Russia, and Research and Education Centre "Molecular Design and Ecologically Safe Technologies" at NSU, Pirogova Str. 2, 630090, Novosibirsk, Russia

Received: September 23, 2009; Revised Manuscript Received: February 16, 2010

Chemically induced dynamic nuclear polarization (CIDNP) and electron paramagnetic resonance (EPR) techniques have been used to study the paramagnetic species formed during the photolysis of the alkaloid lappaconitine and its synthetic analogues in solution. Lappaconitine is a photosensitive antiarrhythmic and hypertension drug, whose major photoproduct (*N*-acetyl anthranilic acid) is also a potent photosensitizer. Both these compounds are lipophilic and might bind efficiently to cell membranes thereby causing phototoxic damage. Photolysis of natural lappaconitine (**I**) as well as its N(20) des-ethyl derivatives (*N*-Bz (**II**), *N*-Me (**III**), *N*-H (**IV**), and *N*(O)-Et (**V**)) results in cleavage of the ester bond with the formation of *N*-acetyl anthranilic acid (**VIII**) and corresponding enamine. The lappaconitine derivative **V** shows maximum photostability which correlates with reference data about its low toxicity. It was shown that the primary reaction step is electron transfer from the amino group to the anthranilic fragment of lappaconitine resulting in an intermediate biradical. The final products are formed via fragmentation of the neutral lappaconitine radicals.

Introduction

Lappaconitine (**I**, Figure 1, R is $-CH_2CH_3$), a diterpene alkaloid extracted from the roots of *Aconitum septentrionale* Koelle, slows the heart rate (bradycardic) and lowers blood pressure (hypotension).[1,2] Diterpene alkaloids which show such antiarrythmic activity can be very toxic and can exhibit phototoxicity.[3−5] Usually, phototoxicity results from the formation of toxic products, mainly active free radicals.[3,6,7] Moreover, in the presence of molecular oxygen, free radicals can produce peroxyl radicals which cause certain types of cancer, atherosclerosis, age-related muscular degeneration, and other diseases.[8] That is why light-induced reactions in biological compounds are of exceptional interest.[3,9−12]

Chemists and pharmacologists have searched for new synthetic analogues of biologically active compounds that exhibit reduced phototoxicity but that retain high therapeutic activity. A quantitative structure−activity relationship (QSAR) study demonstrates a significant dependence of the toxicity of lappaconitine derivatives on their structure.[4] QSAR is the process by which the chemical structure is quantitatively correlated with a well-defined process, such as biological activity or chemical reactivity. We have therefore studied the formation and reactions of free radicals in lappaconitine derivatives.

We report here the chemically induced dynamic nuclear polarization (CIDNP) and electron paramagnetic resonance (EPR) measurements of the phototransformation of the N(20)-des-ethyl derivatives **II**−**V** of lappaconitine (**II** (R = CH_2−Ph), **III** (R = CH_3), **IV** (R = H), **V** (*N*-oxide), Figure 1). Their high sensitivity and selectivity make spin chemistry methods one of the best ways to establish the structure and properties of short-lived paramagnetic intermediates that occur in reactions of biologically relevant compounds.

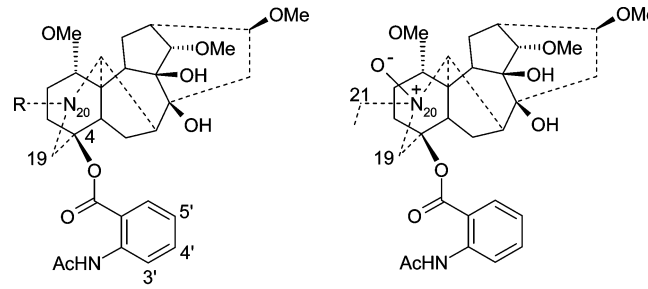

Figure 1. The structure of lappaconitine (**I**, R = CH_2−CH_3) and its derivatives with R = CH_2−Ph (**II**), R = CH_3 (**III**), R = H (**IV**), and *N*-oxide lappaconitine (**V**).

Photoinduced cleavage of natural lappaconitine **I** in solution has been investigated by photo CIDNP methods in our previous studies.[13−15] The analysis of CIDNP effects showed that in the absence of any additives, photodecomposition of lappaconitine occurs with the formation of radical ions and free radicals.[14] The CIDNP effects can occur if the molecular triplet state forms a pair of radicals by intermolecular electron transfer to another ground-state molecule of **I** (stage 1 in Scheme 1) or if the molecular triplet decays to an intramolecular biradical (2) that subsequently undergoes a single intermolecular electron transfer with a ground-state molecule of **I** (3). Both pathways result in the same products **VIII** and **IX** after cleavage of the ester bond in the radical products **VI** and **VII**.[14]

* To whom correspondence should be addressed. Fax: 7-383-3307350; phone: 7-383-3332947; e-mail: polyakov@kinetics.nsc.ru.
† Institute of Chemical Kinetics & Combustion.
‡ University of Alabama.
§ Institute of Organic Chemistry.
# Research and Education Centre "Molecular Design and Ecologically Safe Technologies" at NSU.

10.1021/jp909166r
Published on Web 03/16/2010

SCHEME 1

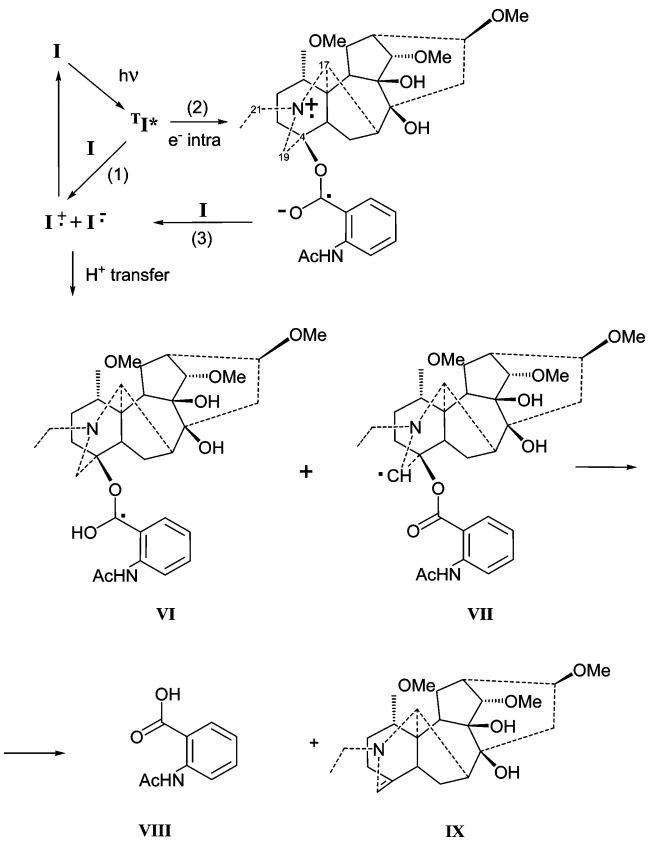

Scheme 1 shows the reaction mechanism of lappaconitine **I** phototransformation suggested from our previous CIDNP data.[14]

In solution, the *N*-acetyl anthranilic acid **VIII** transforms compound **IX** to the imine cation (**X**, R = $-CH_2-CH_3$). The structure of this salt was determined by multinuclear NMR methods (^{13}C, ^{15}N, and ^{1}H).[14]

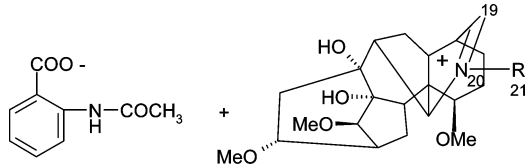

X

The primary reaction step was proposed to be as an intramolecular electron transfer from the amine part of the alkaloid fragment to the anthranilic moiety, which produces a biradical. Unfortunately, it was impossible to prove the formation of a biradical in this reaction using only the signs of the CIDNP effects. The assignment of the mechanism for formation of the initial radical ion pair (RIP) was based only on the CIDNP time dependence.[14] The CIDNP intensity appeared unusually slow in about 20 μs instead of 1−2 μs typical for intermolecular electron transfer.[13]

There are several examples of intramolecular electron transfer, where biradicals are observed in the photolysis of dialkylamino ketones, *N*-acylbenzoate esters, or amine-naphthalene dyad.[16−18] In all cases, the presence of a nitrogen atom in the molecule led to rapid quenching of the excited triplet state with the rate constant about $2-5 \times 10^8$ s^{-1}. The formation of a biradical from γ-amino ketone was attributed to a hydrogen atom transfer from the CH_2-group nearest to the nitrogen atom to the carbonyl group of the ketone. Time-resolved techniques (such as EPR and CIDNP) indicate that the reaction of a tertiary amine with the carbonyl triplet excited state involves sequential electron transfer followed by proton transfer. The deprotonation rates of the amine radical cation falls within the range of 10^8-10^{10} M^{-1} s^{-1} as a function of different polarity and pH[19,20] compared to the bimolecular quenching rate constant (reaction 1 in Scheme 1) 5×10^9 M^{-1} s^{-1}.[13,18]

In the present study, we determine the mechanism of photocleavage of **I** (Scheme 1) in a series of N(20) derivatives **II**−**V** using CIDNP techniques. The reactions proceed by intramolecular electron transfer according to route 2 in Scheme 1. EPR techniques detect the primary biradical at low temperature. We confirm that the amino group N(20) plays a key role in the photolability of lappaconitine and that substitution at the nitrogen atom N(20) (see Figure 1) changes the donor capacity of the amino group and reduces phototoxicity.

Experimental Section

Chemicals. The synthesis of compounds **II**−**V** was carried out according to previously described procedures.[5] Deuterated CD_3OD (Aldrich) was used as supplied. All solutions were prepared with concentrations near 10^{-3} M and were desecrated by Ar bubbling.

Apparatus. For CIDNP experiments, samples in standard 5 mm Pyrex NMR tubes were irradiated directly in the probe of an NMR spectrometer at room temperature. Absorption spectra of compounds **I**−**V** have a maximum wavelength around 300 nm with an extinction coefficient about 5000 M^{-1} cm^{-1}. An EMG 101 MSC Lambda Physik excimer laser was used as the light source (λ = 308 nm, pulse duration 15 ns, average pulse energy 100 mJ). During the photochemical reaction, CIDNP spectra were detected using the DPX 200 Bruker NMR spectrometer (200 MHz ^1H operating frequency). During the time-resolved (TR) CIDNP experiments, standard presaturation techniques were used to suppress the equilibrium signals that occurred with the following pulse sequences: (1) saturating radiofrequency (RF) pulse; (2) laser pulse; (3) time delay; (4) the detecting radiofrequency pulse; and (5) free induction decay. In the TR CIDNP experiments, a 1 μs detecting radiofrequency pulse was used, which is approximately equivalent to a 15° pulse. Quasi steady state (QSS) CIDNP experiments were performed using the special presaturation technique: saturation, 180° pulse, several laser pulses, evolution time, detection pulse, free induction decay. Since the background (equilibrium) NMR signals in the pulse CIDNP experiments were suppressed, only the signals of the products demonstrating nuclear polarization could be observed.[21]

EPR experiments were performed with a Bruker E-680 W/X FT/CW Pulse X-band spectrometer equipped with an MD5EN-W1 dielectric resonator, an Oxford instruments CF935 helium cryostat, and electrically controlled Oxford helium transfer line. The spectrometer is controlled through a Linux workstation with Xepr, the data acquisition and manipulation Bruker software. The samples were prepared in methanol solution (8% of water was added for glass formation) at 1 mM concentration and were irradiated at 77 K with a high-pressure Hg lamp (1 kW) equipped with optical filter (λ > 300 nm).

Results and Discussion

Comparing the ^1H NMR spectra of the photolysis products of compounds **II**−**V** with the spectrum of the imine cation **X** described earlier[15] shows the presence of two compounds with similar structures for imine fragment. For example, Figure 2

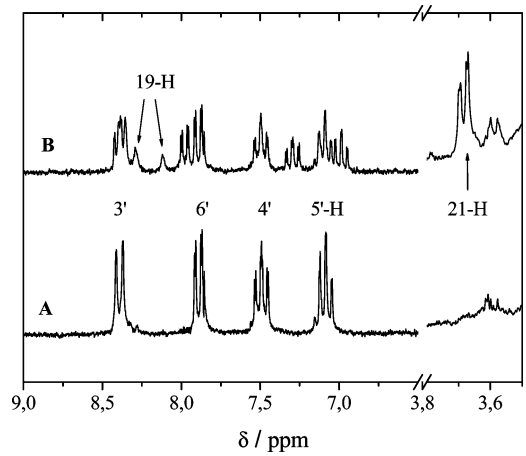

Figure 2. Fragments of ^{1}H NMR spectra of **III** before (A) and after (B) photolysis in CD_3OD. The broad signals at 8.29 and 8.12 ppm correspond to 19-H of **X**, and the two lines at 3.695 and 3.67 ppm correspond to N−CH_3 group of **X**.

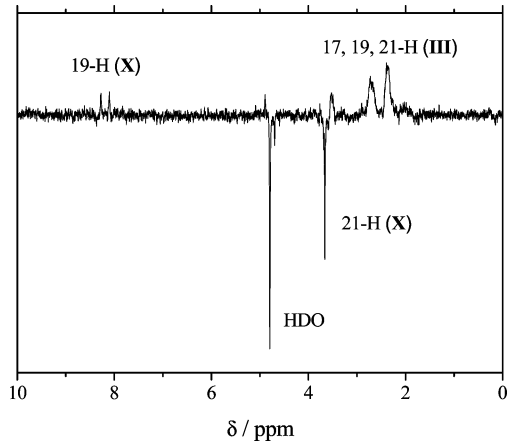

Figure 3. Time-resolved CIDNP spectrum detected after laser irradiation of **III** (1 mM) in CD_3OD with delay time 50 μs between laser and detection pulses.

SCHEME 2

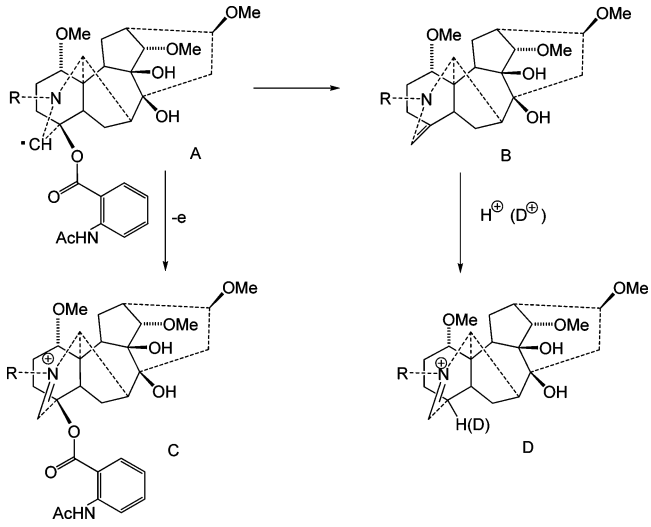

shows the ^{1}H NMR spectra detected before (A) and after (B) photolysis of compound **III** (R = CH_3). The spectrum B in Figure 2 corresponds to a 40% decomposition of the initial compound. There are two signals in the area of the methyl protons connected with nitrogen atom N(20) (two doublets with ratio 3:2, 3.673 ppm and 3.697 ppm, J = 1.3 and 1.2 Hz) and two signals for protons at the 19 position (8.29 and 8.12 ppm) of the imine cation. The imine cation obtained from natural lappaconitine establishes the signal for the 19-H proton at 8.34 ppm.[15]

The possible explanation for the formation of two imine derivatives with similar structures in the reaction under study might be the transformation of radical **A** in two ways (Scheme 2). The first way is the fragmentation of this radical which results in formation of compound **B** following its protonation. The second way is the oxidation of radical **A**. Cation **C** is an analogue of the imine cation **D**.

Additional confirmation of this scheme will be made later during the analysis of the CIDNP effects detected during the photolysis of the lappaconitine derivatives **II**−**IV**.

CIDNP spectra detected during the photolysis of compounds **I**−**IV** exhibit the same type of CIDNP effects. Only the most stable compound **V**, which will be discussed later, is an exception. Analysis of polarization signs allows us to trace the participation of both the radical ions and the neutral radicals in the formation of the final products. Indeed, CIDNP effects detected on the protons of the initial compounds were observed only for the N−CH_2 (or N−CH_3) protons in the time-resolved CIDNP experiments (enhanced absorption at 2.1−3.4 ppm, Figure 3 for **III**). This situation is characteristic for the reversible electron transfer in radical ion pairs with participation of the aliphatic amine radical cations (e.g., triethylamine, $A(CH_2) \sim 3$ mT and $A(CH_3) \sim 0$[20]). In these experiments, we did not observe the polarization of the aromatic protons of the initial compounds. Since the CIDNP intensity is proportional to the value of the hyperfine coupling constant (A) of the corresponding proton in the radical precursor, we propose that polarization of the aromatic protons of the initial compounds and products is absent because of the low values of the hyperfine coupling constants of these protons for the radical anion (0.3−0.5 mT) as compared to the hyperfine coupling constants of the protons in the 19 and 21 positions in the radical cations of the lappaconitine derivatives. Time-resolved (TR) CIDNP spectrum at zero time delay between the laser and the RF pulses shows polarization of only "geminate" products. It was concluded from the TR CIDNP data at zero time delay that enhanced absorption of the initial compounds corresponds to the "cage recombination" product of the triplet radical ion pair (back electron transfer). On the other hand, TR CIDNP spectrum at 50 μs delay demonstrates polarized signals from both "cage" and "escape" products (Figure 3).

On the basis of the assumed structure of the RIP and the rules of CIDNP formation,[22] one might expect that all corresponding protons of the escape products will have opposite polarization compared to the initial compound, namely, emission. However, CIDNP effects for **X** demonstrate different polarization signs for 19-H and 21-H. Positive polarization for 19-H protons of **X** is assumed to be the result of the CIDNP effects formed in the radical pair of the neutral radicals **VI** and **VII**. Indeed, in the radical **VI**, only α-protons, 19-H, have significant hyperfine coupling constants ($A \approx -2.3$ mT). For γ-protons 21-H and 17-H of this radical, by analogy with the triethylamine neutral radical, one might expect $A \approx 0.4$ mT. In this case, according to CIDNP rules for the triplet precursor of the radical pair, positive polarization should be observed for the 19-H of the imine cations **X**, and weak negative polarization should be observed for 21-H of this product. Thus, the polarization of **X** is the superposition of contributions from the

SCHEME 3

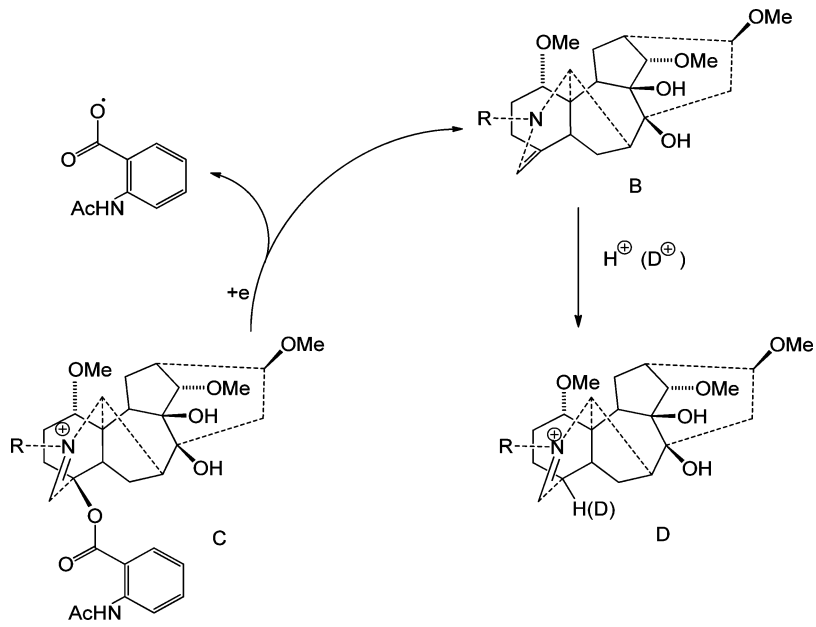

radical ion pair (emission of 19-H and 21-H) and the neutral radical pair (absorption of 19-H and emission of 21-H). The prevalent contribution from the RIP was observed for protons 21-H and 17-H, but for protons 19-H, the contribution from the neutral RP is prevalent.

The most probable source for the polarization of the water molecules (emission, escape product of RIP) in this reaction is the proton exchange with the hydroxyl group of the reaction product, *N*-acetyl anthranilic acid. The polarized proton of the hydroxyl group might show up only as a result of proton transfer from the 19-CH_2 group of the lappaconitine radical cation to the ester fragment of the lappaconitine radical anion. The neutral radical **VI** formed in this reaction can undergo fragmentation with the rate constant $k_{fr} = 4 \times 10^5\ s^{-1}$.[13] The integral intensity of the polarization for water molecules equals approximately one-half of the polarization for 19-CH_2 of the initial lappaconitine. All these results point to the same reaction mechanism for the phototransformation compounds **I**−**IV** (see Scheme 1).

Now, we can return to the discussion of the two products **C** and **D** formed from radical **A** (Scheme 2). First, the difference in the ratio of the CIDNP intensities and the NMR intensities is in accordance with the above suggestion about two ways for product formation. Second, the CIDNP intensities for compounds **C** and **D** are different for derivatives **II**−**V**. We assume that the nature of substitutes at N(20) in these compounds can influence the reaction route (especially the oxidation rate for radical **A**). Third, only one imine cation **D** has been observed after long irradiation time. This fact points to the existence of a channel of transformation from compound **C** to compound **D**. Such a channel can be easily imagined as an electron transfer to the cation **C** followed by fragmentation with formation of the radical of *N*-acetyl anthranilic acid and enamine **B** (Scheme 3). Electron transfer can occur from the lappaconitine excited state.

Next, it is important to discuss the phototransformation mechanism for compound **V** (lappaconitine *N*-oxide), which exhibits the maximum stability. The degree of photocleavage of **V** estimated as the ratio of the yields of reaction products for **V** and **I** after equal irradiation time is approximately 100 times lower. The NMR spectrum of the final product of the phototransformation of **V** coincides with the spectrum detected after photolysis of compound **I**. It was assumed that the first step for the phototransformation of **V** is the cleavage of the N^+-O bond with the formation of compound **I**. Further transformation of **I** occurs via the mechanism described above (Scheme 1) yielding *N*-acetyl anthranilic acid **VIII** and compound **IX**.

As for the possible mechanism for the photoinduced cleavage of the N−O bond of **V**, there are published data for the photoinitiated deoxygenation of the *N*-oxides.[23,24] It was found that UV irradiation and photoinduced interaction of *N*-oxides with carbonyl compounds lead to the formation of *N*-oxide radical cations. It was demonstrated also that *N*-oxide radical cations can form complexes with solvents such as methanol, cyclohexane, or acetonitrile, which then can transform to oxidation products and are accompanied by deoxygenation of the *N*-oxide.[23] This observation suggests that the rate of photolysis of compound **V** is limited by its interaction with a solvent. This result points to the key role that the nitrogen atom N(20) plays in the photolability of lappaconitine derivatives.

EPR Study of Lappaconitine Photolysis at Low Temperature. To detect the primary biradical, lappaconitine was photolyzed at low temperature (77 K), and the sample was analyzed by continuous wave (CW) and pulse EPR techniques. The photolysis of **I** and **III** in methanol glass results in similar EPR spectra because of the combination of spectral lines from the primary biradical and the monoradical. The CW EPR spectrum detected for compound **III** (Figure 4) exhibits a monoradical signal (a) in the middle ($g = 2.0025$) which is most likely due to the lappaconitine radical anion and a four-line signal (b) which is indicative of systems with $S = 1$ and an axially symmetric zero-field splitting tensor ($D \neq 0$, $E = 0$).

The dipolar interaction parameter D provides structural information about triplet species. If two unpaired electrons are well-separated, the value of D can be used to calculate the distance r between two unpaired electrons from the following eq:

$$D = 3g\beta/2r^3 = 1.39 \times 10^3(g/r^3) \qquad (1)$$

Here, D is in mT and r is in Å.[25]

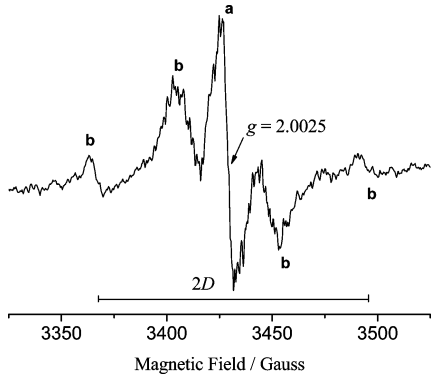

Figure 4. CW EPR spectrum of irradiated lappaconitine **III** in methanol glass. Parameters: modulation frequency, 100 kHz; modulation amplitude, 1.0 G; microwave frequency, 9.6124 GHz; temperature, 77 K.

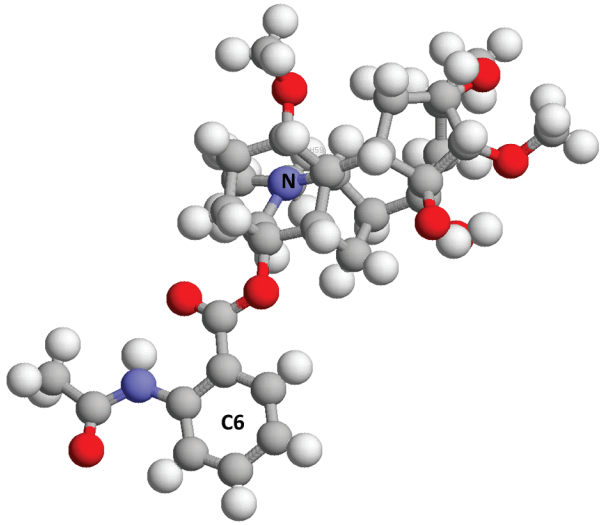

Figure 5. Crystal structure of lappaconitine (adapted from Wang, Y.-P.; Sun, W.-X.; Zhang, J.; Liu, H.-S.; Wen, H.-H. *Acta Crystallogr.* **2007**, *63* (Section E), 1645).

The parameter D estimated from the EPR spectrum (the separation of the outer lines in Figure 4 is $2D$) was 6.4 mT, and the distance r determined from eq 1 for the photogenerated radical pair is 7.6 Å. The estimated r value is consistent with the distance between the nitrogen atom N(20) and the benzene ring C6 (~8 Å) obtained from the crystal structure of lappaconitine (Figure 5). The species, therefore, was attributed to the radical pair where one unpaired electron is localized on the nitrogen atom N(20) and the other one is delocalized over the benzene ring C6. In solution, this distance can be longer or shorter than in the crystal because of the ring C6 rotation.

Also, we made an attempt to include an exchange interaction (J) for distance determination by spectral simulations using the XSophe simulation program. Unfortunately, XSophe does not allow the adjustment of both an isotropic J and a spin−spin dipolar interaction. It varies the J tensor components until a fit occurs resulting in a nontraceless tensor. Therefore, using the separation of the outer high and low field EPR lines and a point dipole approximation, we can provide reasonable accuracy of the distance estimation.

To confirm the formation of a biradical in the irradiated lappaconitine solution, we carried out a nutation experiment based on dynamic phase shifts[26] using the PEANUT (phase-inverted echo-amplitude detected nutation) technique developed by Stoll et al.[27] The experiment was performed at 20 and 60 K.

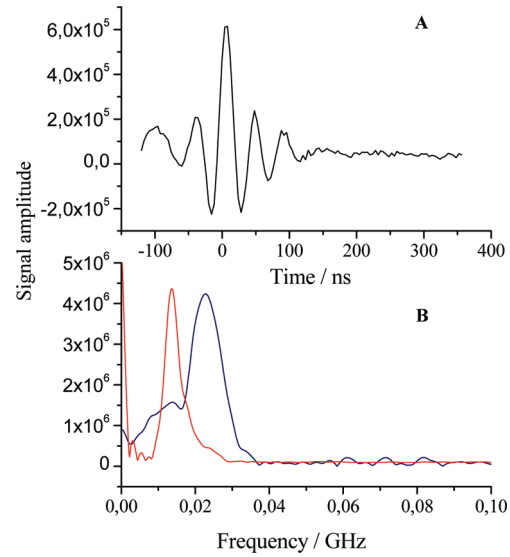

Figure 6. (A) Nutation experiment based on dynamic phase shifts using the PEANUT technique performed at 20 K for irradiated lappaconitine solution in MeOH. Experimental parameters: magnetic field position, 3470 G; microwave frequency, 9.7563 GHz; τ-value, 460 ns; SRT = 800 ms. (B) Fourier transform of the nutation experiment: (red) diamond, (blue) lappaconitine.

Similar spectra were obtained at both temperatures. Figure 6A shows the time domain spectrum of lappaconitine. For comparison, we carried out nutation measurements of the standard diamond sample with known spin number ($S = 1/2$) under the same experimental conditions. Figure 6B exhibits a Fourier transform of the nutations for diamond and lappaconitine (unknown spin number, most likely $S > 1/2$).

The pulse sequence for the PEANUT experiment is a two-pulse primary pulse sequence with the refocusing π pulse replaced by a special composite nutation pulse. After a first microwave $\pi/2$ pulse, the transverse magnetization evolves and dephases during the evolution period τ. Then, a nutation pulse of constant length T is applied. This pulse is subdivided into two parts of variable length t and $T - t$ with opposite microwave phases 0 and π. After the nutation pulse, the spins again freely evolve and form a primary echo at time τ.

From Figure 6B, we can determine values of the nutation frequencies for lappaconitine and diamond at the positions of their peaks. The observed signals and their nutation frequencies are complicated functions of the **g**-tensors, hyperfine (**A**), quadrupole (**Q**)-tensors, zero field parameters (**D**), the vectors $\mathbf{B_0}$ and $\mathbf{B_1}$, and the changes of the magnetic quantum numbers Δm_S and Δm_I that characterize a particular transition. The nutation frequency is useful for identification of the transitions.

The spin Hamiltonian for systems with electron spin S and nuclear spin I is described as

$$H = H_0 + H_1$$

Here, H_0 is static Hamiltonian and H_1 is perturbation.

$$H_0 = H_{EZ} + H_{NZ} + H_{ZFS} + H_{HFS} + H_{NQ} = \beta_e \mathbf{B}_0 g S/\hbar + \beta_n \mathbf{B}_0 g I/\hbar + S\mathbf{D}S + S\mathbf{A}I + I\mathbf{Q}I$$
$$H_1 = 2\beta_e \mathbf{B}_1 g S/\hbar$$

The nutation frequency depends on a ratio between the terms H_{ZFS} and H_1 (interaction with variable magnetic field). There are two limiting cases:

1. In the case of strong microwave field, $H_{ZFS} \ll H_1$, all the transitions of the multilevel spin system are excited simultaneously and the nutation frequency is

$$\Omega_n = \omega_1 = \gamma B_1$$

2. In the case of weak microwave field, $H_{ZFS} \gg H_1$, only the transition $|S, m_s - 1\rangle \leftrightarrow |S, m_s\rangle$ of the multilevel system with spin S is resonantly excited, and the nutation frequency is determined by the relation

$$\Omega_n = \sqrt{S(S+1) - m_s m_s'} \times \omega_1 \quad (2)$$

$$m_s' = m_s - 1$$

$$\sqrt{S(S+1) - m_s m_s'} = C \quad (3)$$

$$\Omega_n = C\omega_1 \quad (4)$$

According to eqs 2−4, knowing the nutation frequency, one can determine the spin quantum number and can identify a quantum transition. The ω_1 value was calculated from eq 2 using the diamond spin number $S = 1/2$. Since for $S = 1/2$ and $m_s' = \pm 1/2$, $C = 1$, $\omega_1 = \Omega_n$ for the diamond. Then

$$C(\text{lappaconitine}) = \Omega_n(\text{lappaconitine})/\Omega_2(\text{diamond}) \quad (5)$$

The nutation frequency of lappaconitine was taken from the experiment (Figure 6B, blue). Using eq 5, the calculated C value was 1.45 ± 0.2. This value is close to $\sqrt{2} = 1.41$ which corresponds to spin state $S = 1$ and $m_s = \pm 1, 0$. The observed EPR signal could not be from the triplet excited state since the lifetime of the triplet state for the ethers of anthranilic acid are in the range of a few seconds even at low temperatures.[28] All of the molecular excited states would have decayed by radiation before the CW EPR measurements were made. Thus, the triplet state here is from a ground-state radical pair. Therefore, the EPR study confirms that the lappaconitine biradical is formed during photolysis as a primary reaction step.

Conclusion

All N(20) substituted lappaconitine derivatives, which are considered as the potential bradycardic and hypotensive drugs, show high photochemical activity except the lappaconitine *N*-oxide. Lappaconitine *N*-oxide shows the maximum photostability (at least 2 orders slower photodegradation rate). Compound **V** also demonstrates very low toxicity in vivo.[29] The photolysis of **I**−**V** results in a cleavage of the ester bond with elimination of the *N*-acetyl anthranilic acid. The reaction starts with intramolecular electron transfer followed by the formation of radical ions as well as neutral radicals of lappaconitine. This might be the reason for the high phototoxicity of lappaconitine. The anthranilic moiety plays the role as a chromophore in the molecule, and its high reactivity is determined by the N-function which functions as an electron donor. Identifying the reaction mechanism for the photolysis of these compounds may be helpful in discovering the biogenesis of the aconitum-type diterpene alkaloids. In the present study, the possibilities and advantages of physical methods (CIDNP, chemically induced dynamic nuclear polarization, and pulsed EPR) in the investigation of free-radical intermediates of biologically active compounds were demonstrated.

Acknowledgment. This work was supported by grants 07-03-00583 and 08-03-00372 of Russian Foundation of Basic Research, by grant CRDF RUXO-008-NO-06, and by the U.S. National Science Foundation for EPR Instrument grants CHE-0342921 and CHE-0079498. The authors thank Prof. Michael Bowman (The University of Alabama) for editorial assistance and Prof. Bowman and Dr. Marina Samoilova (Institute of Chemical Kinetics and Combustion, Russia) for kind help with the EPR experiments.

References and Notes

(1) Turabekova, M. A.; Rasulev, B. F. *Molecules* **2004**, *9*, 1194.
(2) Heubach, J. F.; Schuele, A. *Planta Med.* **1998**, *64*, 22.
(3) Quintero, B.; Miranda, M. A. *Ars Pharm.* **2000**, *41*, 27.
(4) Dzhakhangirov, F. N.; Sultankhodzhaev, M. N.; Tashkhodzhaev, B.; Salimov, B. T. *Chem. Nat. Compd. (Engl. Transl.)* **1997**, *33*, 190.
(5) Pankrushina, N. A.; Nikitina, I. A.; Anferova, N. V.; Osadchii, S. A.; Shakirov, M. M.; Shults, E. E.; Tolstikov, G. A. *Russ. Chem. Bull. Int. Ed.* **2003**, *52*, 2490.
(6) *The Photostability of Drugs and Drug Formulations*; Tonnesen, H. H., Ed.; Taylor & Francis: London, 1996.
(7) Thomas, S. E.; Wood, M. L. *Br. Med. J.* **1986**, *292*, 992.
(8) Langseth, L. *Oxidants, antioxidants and disease prevention*; International Life Science Institute: Belgium, 1996.
(9) Castell, J. V.; Gomez-Lechon, M. J.; Hernandez, D.; Martinez, L. A.; Miranda, M. A. *Photochem. Photobiol.* **2008**, *60*, 586.
(10) Greenhill, J. V.; McLelland, M. A. *Prog. Med. Chem.* **1990**, *27*, 51.
(11) Greenhill, J. V. In *The Photostability of Drugs and Drug Formulations*; Tonnesen, H. H., Ed.; Taylor & Francis: London, 1996; pp 83−110.
(12) Glass, B. D.; Brown, M. E.; Drummond, P. M. In *Drugs: Photochemistry and Photostability*; Albini, A., Fasani, E., Eds.; Royal Society of Chemistry: Cambridge, U.K., 1998; pp 134−149.
(13) Polyakov, N. E.; Khan, V. K.; Taraban, M. B.; Leshina, T. V.; Luzina, O. A.; Salakhutdinov, N. F.; Tolstikov, G. A. *Org. Biomol. Chem.* **2005**, *3*, 881.
(14) Polyakov, N. E.; Leshina, T. V. *Russ. Chem. Bull. Int. Ed.* **2007**, *56*, 631.
(15) Polyakov, N. E.; Leshina, T. V.; Tkachev, A. V.; Nikitina, I. A.; Pankrushina, N. A. *J. Photochem. Photobiol., A: Chem.* **2008**, *197*, 290.
(16) Wagner, P. J.; Kemppainen, A. E.; Jellinek, T. *J. Am. Chem. Soc.* **1972**, *94*, 7512.
(17) Wagner, P. J.; Siebert, E. J. *J. Am. Chem. Soc.* **1981**, *103*, 7335.
(18) Abad, S.; Pischel, U.; Miranda, M. A. *Photochem. Photobiol. Sci.* **2005**, *4*, 69.
(19) Goez, M.; Sartorius, I. *J. Phys. Chem. A* **2003**, *107*, 8539.
(20) Saluberlich, J.; Brede, O.; Beckert, D. *J. Phys. Chem. A* **1997**, *101*, 5659.
(21) Goez, M. *Concepts Magn. Reson.* **1995**, *7*, 263.
(22) Kaptein, R. *Chem. Commun.* **1971**, 732.
(23) Koldasheva, E. M.; Geletii, Y. V.; Yanilkin, V. V.; Strelets, V. V. *Russ. Chem. Bull.* **1990**, *5*, 994.
(24) Geletii, Y. V.; Kuzmin, V. A.; Levin, P. P.; Shafirovich, V. Y. *React. Kinet. Catal. Lett.* **1988**, *37*, 307.
(25) Eaton, S.; More, K. M.; Sawant, B. M.; Eaton, G. *J. Am. Chem. Soc.* **1983**, *105*, 6560.
(26) Bowman, M. K. In *Modern Pulsed and Continuous-Wave Electron Spin Resonance*; Kevan, L., Bowman, M. K., Eds.; Wiley: New York, 1990.
(27) Stoll, S.; Jeschke, G.; Willer, M.; Schweiger, A. *J. Magn. Reson.* **1998**, *130*, 86.
(28) Beeby, A.; Jones, A. E. *Photochem. Photobiol.* **2000**, *72*, 10.
(29) Tolstikova, T. G.; Voevoda, T. V.; Dolgikh, M. P. *Eksp. Klin. Farmakol. [Article in Russian]* **2001**, *4*, 7.

JP909166R